Hindawi
Advances in Civil Engineering
Volume 2019, Article ID 7513645, 10 pages
https://doi.org/10.1155/2019/7513645

Research Article

Numerical Analysis for U-Shaped Thin-Walled Structure Reinforced Timber Beam Based on Thin-Layer Beam Theory

Hui Liu,[1] Jun Hu ,[2] Guohui Li,[1] and Guangying Mo[1]

[1]*Architectural Design and Research Institute of Guangdong Province, Guangdong, China*
[2]*College of Civil Engineering and Architecture, Hainan University, Haikou 5702228, China*

Correspondence should be addressed to Jun Hu; hj7140477@hainu.edu.cn

Received 5 November 2018; Revised 18 December 2018; Accepted 23 December 2018; Published 10 February 2019

Academic Editor: Evangelos J. Sapountzakis

This paper presents a theoretical model, taking into account the shear deformation subjected to the influence of U-shaped member by geometric parameters as flange height based on thin-layer beam theory, to analyze the structural bending behavior of U-shaped member reinforced timber composite beams, and the feasible design forms of U-section have been pointed out. The algorithm for this composite beam is the most practical and effective method to meet the accurate solution. The formulas for the common forms of U-section are presented. It aims to develop a rational engineering approach. The proposed model has been validated by comparing the results obtained in the present analysis with experimental results and finite element analysis. Furthermore, the results suggested that the value of flange height can be one-fifth the beam height based on the present analysis by comparison of two types of beams. And it is shown that the model provided here correlates consistently and satisfactorily with a wide range of timber beams reinforced by a thin-walled structure such as steel or aluminum alloy sheet bonded to their tension faces.

1. Introduction

Timber structures' natural features are attractive in applied engineering. As timber structures are brittle materials, different reinforcement techniques can be adopted for avoiding easily damageable parts of the building, such as concrete, steel, and FRP used for timber beams and sandwich beams [1–7]. However, the reinforcements often make beam confront stiffness degradation and bonded layers separation due to interlay slip associated with flexibility and deformation of connectors [8–10]. Shear stress plays a significant role in bending strength of composite beam as discussed in many research studies, and some numerical methods to estimate it have been established [5, 9, 11–16]. Malek et al. proposed that shear stress in the interface of concrete and plate beams leads to flexural cracks compared to other items including tensile stress, analytically given by unique definition from high-order ordinary differential equations applied to the concrete beam [17].

A system of U-shaped member provided to reinforce timber beam shows a ductile behavior with respect to the plate [18–20]. The materials such as steel, aluminum, cement asbestos, and GFRP adopted are all available [21]. And, a U-shaped member using GFRP fabric was first discussed by Theakston [22].

Many publications [11, 12, 23, 24] reported that using the U-shaped member can effectively improve the maximum bending capacity. Rescalvo et al. [19, 20] presented data to demonstrate the benefits in flexural strength, and stiffness of timber improved due to the U-shaped member [19, 20]. The same results were obtained with applications of the U-shaped member reinforced LVL beam in a study by Subhani et al. [25]. The improvements of 15.94% and 16.10% in flexural strength and stiffness, respectively, were observed from the experiment comparison [25].

Until now, various multilayered composite beam theories have been developed by many authors [26–31]. Several exact mathematical solutions were established based on the concepts of Timoshenko beam theory, including displacement-based theory, first-order shear deformation theory, and higher-order theory [32]. Alternatively, Edward and Thomas [2] developed a plate theory to reflect the mechanical behavior

of thin-layer composite structures shown by the model without externally imposed shear force in the cross section of thin layer [2]. Based on the plate theory, Hussein has completed analytical and experimental studies that give a calculated simulation focussed on the influence of the adhesive [9]. Recently, the plate theory was used in the thin-walled steel to strengthen timber composite structures [33].

The current study for simulating the flexural behavior of the U-shaped member reinforced composite beam mainly adopted the method calculating the strain relation based on the Bernoulli's principle [6, 18]. Subhani et al. [25] presented an algorithm to be more accurate with a nonlinear model [25]. However, both simulations related to the experiment were given by available literature, and this method works by neglecting the transverse shear strains completely defined by the model considering the balance of compressive and tensile forces.

In this paper, the mechanical behavior of the timber beam was reinforced with the U-shaped member as the thin-walled plate made in the steel plate or aluminum alloy strip unlike the composite beam reinforced by two parts fully glued. The method estimating the bending capacity cannot adequate to fit the principle, and so the research was presented to analysis based on thin-layer beam theory. The steel plate or aluminum alloy is widely used in engineering; notwithstanding that FRP has advantages of high tensile strength with easily moldable properties, but the premature catastrophic failure of FPR could easily occur by wood splinters when used in the composite beam [23]. This paper will show the bending capacity of U-shaped thin-walled member reinforced timber beam by the plate theory. The approach will be prescribed and compared with the thicker composite beams [34–36]. It will be applied to reflect correctly the potential function of U shape in terms of bending capacity and stiffness with respect to the layer slip or shear displacement.

2. Analytical Models

Several exact mathematical analytical solutions of displacement and stress for composite beams with different combinations have been presented in the professional literature.

In general, two different approaches have been adopted to study composite beams: thick-layer beam theories and thin-layer beam theories. In thicker layer beam theory approaches, researchers wanted to overcome connect issues and explain the behaviors of composite structures more accurately, which is known by the beam being inherently subjected to transverse shear between the sections. Girhammar et al. [36] presented the internal actions and established the first- and second-order models with respect to the slip effect deflection. Nie et al. [37], based on the uniform loading, have proposed the stiffness reduction method in deflection analysis. Girhammar and Gopu [38] presented an exact procedure using two second-order ordinary differential equations in terms of interlayer slip for calculating deflection of composite beams [37, 38]. In thin-layer beam theory approaches, mainly known as sandwich construction in the form of thin face panels, the analytical model and solution to estimate the effective mechanical properties of adhesives are unavoidable. Theoretical studies about the bending capacity subjected to various working loads have been given, and the research on nonrigid adhesive applied the plate theory developed by Hussein [1, 2, 9, 39, 40]. In fact, the approaches were initiated by the Kirchhoff–Love plate theory.

2.1. Mechanical Model. Due to the highly nonlinear behavior of timber joints, fasteners such as screws are potentially ductile in nature compared with glued joints and carpenter joints. Under compressive stresses, steel or aluminum alloy plate used for reinforced timber can be loaded far over its elastic limit and be able to deform in a distinctly plastic manner, especially the aluminum alloy performs corresponding with timber in terms of mechanism properties behavior.

For a thin-layer beam, the basic structural principle is that the facings act together to resisting moment counteracting the external imposed bending moment. Figure 1 depicts the isolation unit which shows that moment is constant through the thickness, and the core resists the shear stresses set up by the external loads. In Figure 1, $q(x)$ are external loads, $P(x)$ represents the bonding force between two sections, and V_i is the value of shear owing to the facings act. Then, M_i and N_i are bending moment and tensile with isolation units. This kind of theory's model defines a structural sandwich covered by a thin sheet as a major contributor to tensile strength [41]. The isolation unit of thick-layer beam model as two isolated beams connected together by the adhesive is shown in Figure 2. Especially, the moment M_1 is different from M_2 by each part, but in Figure 1, the value of moment M_1 is about equal to M_2 with the thin layer.

For verifying the reliability of the design models of U-shaped plate reinforced timber beam, De la Rosa et al. have analyzed them using the transformed section method and the section conditions of equilibrium. De la Rosa et al. have presented theory based on the formula derived from stress-strain relationship of materials and the conditions of equilibrium with Bernoulli's principle. However, the estimate method was checked with the results obtained experimentally on reinforcement of FPR [18]. A different calculation method to simulate the U-shaped plate as reinforcement based on Shen's work was presented, which is translated from the thick-layer beam theory and displayed based on adding the contribution of U-section strength to the element without strengthening, while the reinforcement material is steel plate in concrete beam [42]. U section is nonrigid adhesive on the tension face of the timber beam and owed the property of self-supporting due to the unwrapped form and is also weaker in free edge under compressive force caused by the nonbonded adhesive flange of the U section in the lateral sides of the beam. Thus, the thin-layer beam may be necessary and sufficient to reflect the mechanical simulation of timber beam assembled by a U-shaped member in such kinds of material properties.

The formulation of the planar two-layer composite beam model uses the following assumptions: (1) the materials are

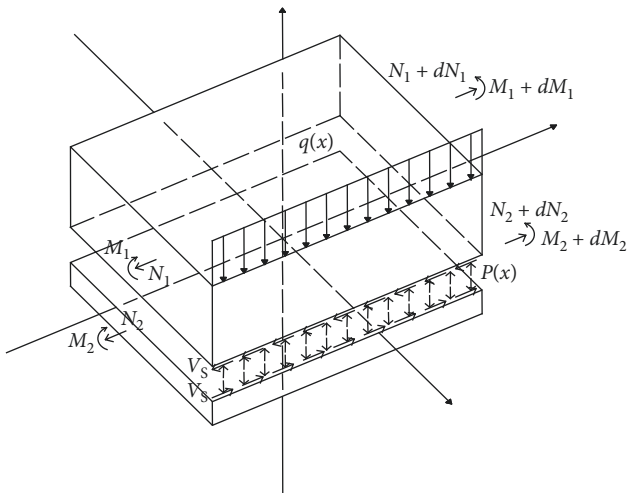

Figure 1: The isolation unit of the thin-layer beam.

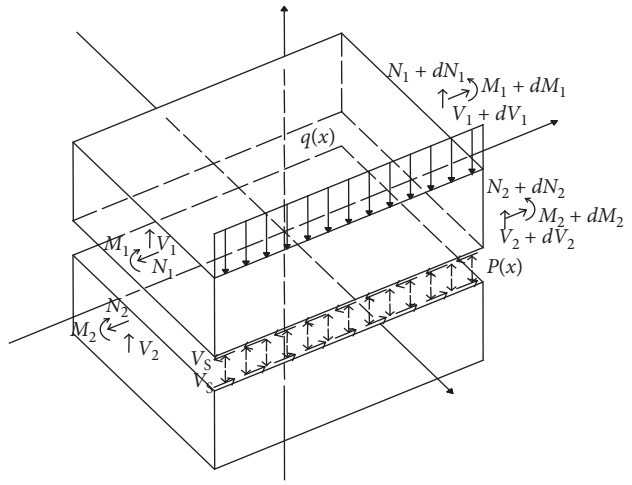

Figure 2: The isolation unit of the thick-layer beam.

orthotropic and linear elastic; (2) the U-shaped layer is symmetrical with respect to the plane of deformation and forces, and the layers are continuously connected only on the bottom of beam; and (3) the faces are thin in comparison with the core depth. This implies that the flexural rigidity of each face about its own middle surface is negligible, and consequently, the inplane stresses resisted by each skin are uniformly distributed across its thickness.

A distribution of U-shaped reinforcement is shown in Figure 3, which is fabricated by attaching timber to the web part of the U-section. The tensile force obviously generates from the connection between the surfaces of two parts. There are loads which result in bending with the effect of U-section warping, such as the shear stress between interlayers and the friction both on web and flange between the timbers and due to the shear displacement lead by the distortion that induces influence of the extent to which the plane sections remain oriented after bending.

2.2. Shear Displacement Analysis. An interlayer slip often develops if it is up to sufficient magnitude and therefore

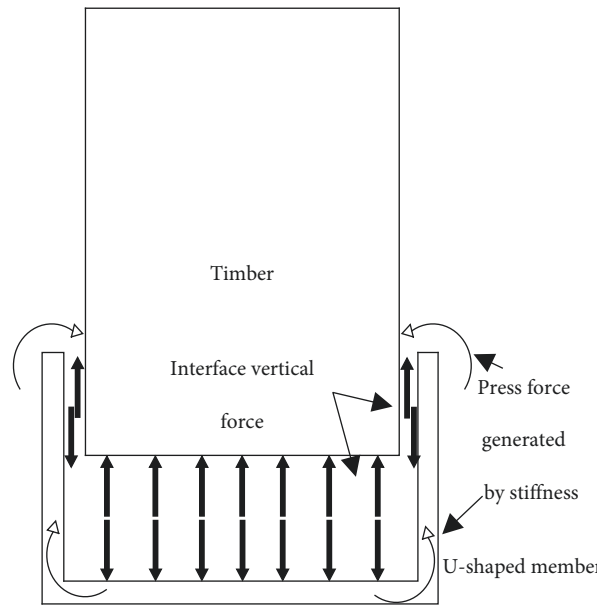

Figure 3: The mechanics model in cross section of U-section combined with timber beam.

affects significantly the deformation and the stress distribution of the composite system. The plate assembled to timber beam having finite stiffness, because of distortion, contributes most to any unequal displacement of the plate and the lower face of the timber with interlayer slip under edgewise loads, as assumed in the model of Figure 4. The U section can not only hold off vertical tensile force P by connectors but also prevent the shear slip by the strengthening function of the flange. The friction horizontally distributed between plane flange and timber functionally resists partial interaction especially contributed to the force induced by edgewise warping, works together with reinforcement of connector at the bottom of the beam and with extrusion forces generated by the U-section, and plays the role of supplementary stress as well as friction vertically transferred by lateral interfaces.

3. Numerical Analysis

3.1. U-Shape Simulation Based on the Thin-Layer Beam Theory. The elemental longitudinal section of a prismatic rectangular beam integrates with the U-shaped member under uniformly distributed load along a beam of length L and the total load given by Q. The distance between centroids of principal moment-carrying member h is shown in Figure 3. Considering the interlayer effects of shear bonding stiffness, defined as α, the second-order differential equation [2] for the shear stress τ and deflection ω can be expressed as follows:

$$\frac{d^2\omega}{dx^2} - \frac{h}{\alpha^2 EI_0}\frac{d\tau}{dx} = -\frac{M}{EI_\infty}, \tag{1}$$

$$\frac{d^2\tau}{dx^2} - \alpha^2\tau = -\frac{\alpha^2}{h}\left[1 - \frac{EI_0}{EI_\infty}\right]V, \tag{2}$$

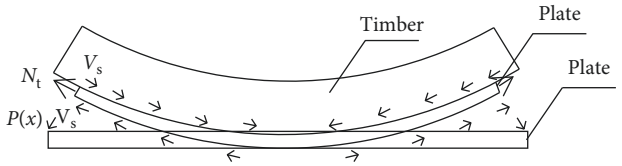

Figure 4: The mechanics model of bond-slip behavior between interface of steel and timber.

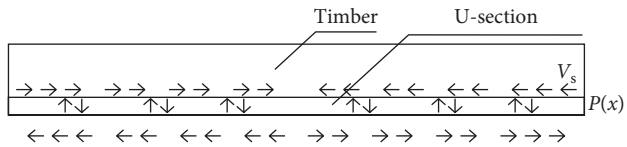

Figure 5: The mechanics model of bond-slip behavior between interface of "U"-shaped steel and timber.

where EI_0 is the stiffness of all beam parts as if unglued and EI_∞ is the stiffness of composite beam if parts were glued together; the bending moment and shear load at a point located at distance x from a reaction are calculated as follows:

$$M = \frac{Q}{2}x - \frac{Q}{2L}x^2, \tag{3}$$

$$V = \frac{Q}{2} - \frac{Q}{L}x. \tag{4}$$

Substituting the expression for V given in equation (4) into equation (2),

$$\tau = A\cosh \alpha x + B\sinh \alpha x + \frac{1}{h}\left[1 - \frac{EI_0}{EI_\infty}\right]V. \tag{5}$$

Constants of integration A and B are evaluated using the following boundary conditions; the boundary conditions are evaluated at $x = 0$ and $x = L/2$, where the length of 0 represents the ends of the beam and half of span represents the midspan of the beam. At points, $d\tau/dx = 0$ or $\tau = 0$, can be shown by Equation (6):

$$\begin{aligned} x &= 0, \\ \frac{d\tau}{dx} &= 0, \\ x &= \frac{L}{2}, \\ \tau &= 0. \end{aligned} \tag{6}$$

Using the above boundary conditions, the following expressions for A and B can be obtained:

$$B = \frac{Q}{\alpha Lh}\left[1 - \frac{EI_0}{EI_\infty}\right], \tag{7}$$

$$A = -\frac{Q}{\alpha Lh}\left[1 - \frac{EI_0}{EI_\infty}\right]\tanh\frac{\alpha L}{2}. \tag{8}$$

By substituting equations (7) and (8) into equation (5), the shear stress is expressed as

$$\tau = \frac{Q}{h}\left[1 - \frac{EI_0}{EI_\infty}\right]\left[\frac{1}{\alpha L}\sinh \alpha x + \frac{1}{\alpha L}\tanh\frac{\alpha L}{2}\cosh \alpha x + \frac{1}{2} - \frac{x}{L}\right]. \tag{9}$$

Due to the strain obtained in equation (9), the maximum deflection $\omega_{\max}$ which under the total compressive Q with integration and evaluation of integration constants leads to

$$\omega_{\max} = \frac{5QL^3}{384EI_\infty}\left\{1 + \frac{12}{5}\left(\frac{EI_\infty}{EI_0} - 1\right)\left(\frac{2}{\alpha L}\right)^2 \cdot \left[1 - 2\left(\frac{2}{\alpha L}\right)^2\left(1 - \frac{1}{\cosh(\alpha L/2)}\right)\right]\right\}, \tag{10}$$

where

$$\alpha^2 = \frac{h^2K}{EI_\infty - EI_0}\left(\frac{EI_\infty}{EI_0}\right), \tag{11}$$

$$EI_\infty = EI_0 + EA \cdot h^2, \tag{12}$$

$$EI_0 = E_1I_1 + E_2I_2, \tag{13}$$

$$\frac{1}{EA} = \frac{1}{E_1A_1} + \frac{1}{E_2A_2}, \tag{14}$$

where K is defined as shear modulus of adhesive or shear load per unit span length to cause unit slip.

In a similar manner, an expression for the midspan deflection fulfills other load position conditions that can be obtained, and the function W obtained to represent the constant of integration is given by

$$W = \frac{k(3 - 4k^2)QL^3}{48EI_\infty}\left\{1 + \frac{6}{(3 - 4k^2)}\left(\frac{EI_\infty}{EI_0} - 1\right)\left(\frac{2}{\alpha L}\right)^2 \cdot \left[1 - \frac{\sinh \alpha kL}{\alpha kL\cosh(\alpha L/2)}\right]\right\}, \tag{15}$$

where k is the load position.

Based on the graphs [2, 9], and by taking α into numerical evaluation for the parametric study, $\omega_{\max}$ always increase inducing values of $\alpha L/2$ decrease when EI_∞/EI_0 remains increasing proportionally.

A parameter χ which represented constant coefficient under different forms of load distribution is used in the various expressions in the interests of brevity. The results can be simplified according to equations (10), (16), and (17) with a function $\Delta\kappa$ which reflected reactions between the interfaces of the elements.

The thin-layer beams in equation (10) describe the result that can be represented through a function W as

$$W = \chi(\Delta\kappa + 1)\frac{QL^3}{EI_\infty}. \tag{16}$$

The function $\Delta\kappa$ is denoted as equation (17) due to different models in terms of the different loading modes:

For the first case in equation (16),

$$\Delta\kappa = \frac{6}{(3-4k^2)}\left(\frac{EI_\infty}{EI_0}-1\right)\left(\frac{2}{\alpha L}\right)^2\left[1-\frac{\sinh\,\alpha kL}{\alpha kL\,\cosh(\alpha L/2)}\right], \tag{17}$$

where $\Delta\kappa$ is calculated in the term under the offset point load.

It can be seen that parameter α in equations (17), (22), and (23) significantly determines the function $\Delta\kappa$ contributing to midspan deflection.

3.2. Thick-Layer Beam. This method is to simulate the composite beam by second-order shear deformation theory presented [43]. It assumes that the displacement u has a cubic variation through the thickness of each section, with moment differential equations of equilibrium for beams considering corrected shear force with respect to slip effects. The resulting equations for midspan deflection of the beam under uniformly distributed load are given as follows:

$$\omega_{\max} = \frac{5QL^3}{384EI_\infty} + \frac{Q}{\alpha^4 EI_\infty}\left\{\left(\frac{EI_\infty}{EI_0}-1\right)\left[\frac{1}{\cosh(\alpha L/2)}+\frac{\alpha^2L^2}{8}-1\right]\right\}. \tag{18}$$

Likewise, under offset point, the load is given as

$$\omega_{\max} = \frac{QL^3}{48EI_\infty}+\frac{Q}{\alpha^3 EI_\infty}\left(\frac{EI_\infty}{EI_0}-1\right)\left[\frac{\alpha L}{4}-\frac{\sinh^2(\alpha L/2)}{\sinh\,\alpha L}\right], \tag{19}$$

in all of which

$$\alpha^2 = \frac{h^2K}{EI_\infty - EI_0}\left(\frac{EI_\infty}{EI_0}\right), \tag{20}$$

and the thick-layer beams in equations (18) and (19) can be simplified by

$$W = \chi\frac{QL^3}{EI_\infty}+\Delta\kappa\frac{Q}{EI_\infty}. \tag{21}$$

For the second case in equation (21),

$$\Delta\kappa = \frac{1}{\alpha^3}\left(\frac{EI_\infty}{EI_0}-1\right)\left[\frac{\alpha L}{4}-\frac{\sinh^2(\alpha L/2)}{\sinh\,\alpha L}\right], \tag{22}$$

where $\Delta\kappa 2$ is calculated in the term under the uniformly distributed load:

$$\Delta\kappa = \frac{1}{\alpha^3}\left(\frac{EI_\infty}{EI_0}-1\right)\left[\frac{\alpha L}{4}-\frac{\sinh^2(\alpha L/2)}{\sinh\,\alpha L}\right]. \tag{23}$$

In the two cases, the general expressions for displacement are presented, all for a simply supported beam. It can be seen that the algorithms formed in two cases are different shown by the relationships of $\Delta\kappa$ with fundamental function $\chi(QL^3/EI_\infty)$. The thin-layer theory's simplified expression of W contains the $\Delta\kappa$ as argument in $\chi(QL^3/EI_\infty)$ function calls. The thick-layer theory's expression contains the $\Delta\kappa$ representing the intercept with respect to $\chi(QL^3/EI_\infty)$. Equation (26) can be obtained by

$$\theta = -((M + N_1\cdot \mathrm{H})/EI_0), \tag{24}$$

$$\Delta\mu' = \left(\frac{N_1}{E_1A_1}-\frac{N_2}{E_2A_2}-\theta H\right), \tag{25}$$

$$\Delta\mu'' - \alpha^2\Delta\mu = (V\cdot H/EI_0), \tag{26}$$

where M is the bending moment, N is the axial force, V is the external shear force, i represents each part, and H is the height of the beam. When neglecting external shear force, the method assumes to be applied to simulate the thin-layer model by equations (24)–(26); the results to be calculated are

$$\frac{N_1}{E_1A_1} = \frac{N_2}{E_2A_2}. \tag{27}$$

It can be seen that the both sides of equation (27), a set of axial interface force, commensurate with extensional stiffness of each parts leading to balancing themselves; that is, the equation obtained a solution that has no value to concern in this way. It means that the equation for two cases could not be interchanged for calculation of composite beam in two forms. Numerical and mechanical analysis are done to illustrate the effectiveness and efficiency of adopting thin layer beam theory for numerical analysis of the U-shaped member composite timber beam without losing any generality, there are insignificant effects to interlayer shears, but the face normal stress presents greater sensitivity to the variation of bond stiffness value as researches [9, 17] have shown. In principle, increased bond stiffness induces increased face normal stress. The same function implies that adopting expressions is reasonable due to the absence of loads which were induced by flange assuming an advantage in the remaining composite beam bearing the load together herein.

3.3. Finite Element Analysis. This work was not aimed at identifying the relationship of load and slip deflection for the composite structure but rather to analyze the flexural behavior strengthened by the U-shaped member provided. Here, the load-displacement plot for models of bending capacity simulation with regard to the height of flange was obtained with two types of the composite beam containing two kinds of materials for U-shaped member: one is steel and the other is aluminum alloy. The finite element analysis based on experiments shown in Figure 6 will be discussed further.

The U-shaped member in steel is an SU-OT beam according to data of L-1 [44], while the AU-T beam is an aluminum alloy U-shaped sheet-timber composite beam; the main mechanical properties of aluminum alloy are $f_t = 206$ MPa, $E = 0.7\times10^5$ MPa, and $\gamma = 0.34$; the values of timber according to the test of *Pseudotsuga menziesii* wood are $f_c = 28.32$ MPa, $E = 11003$ MPa, and $\gamma = 0.3$, where E is

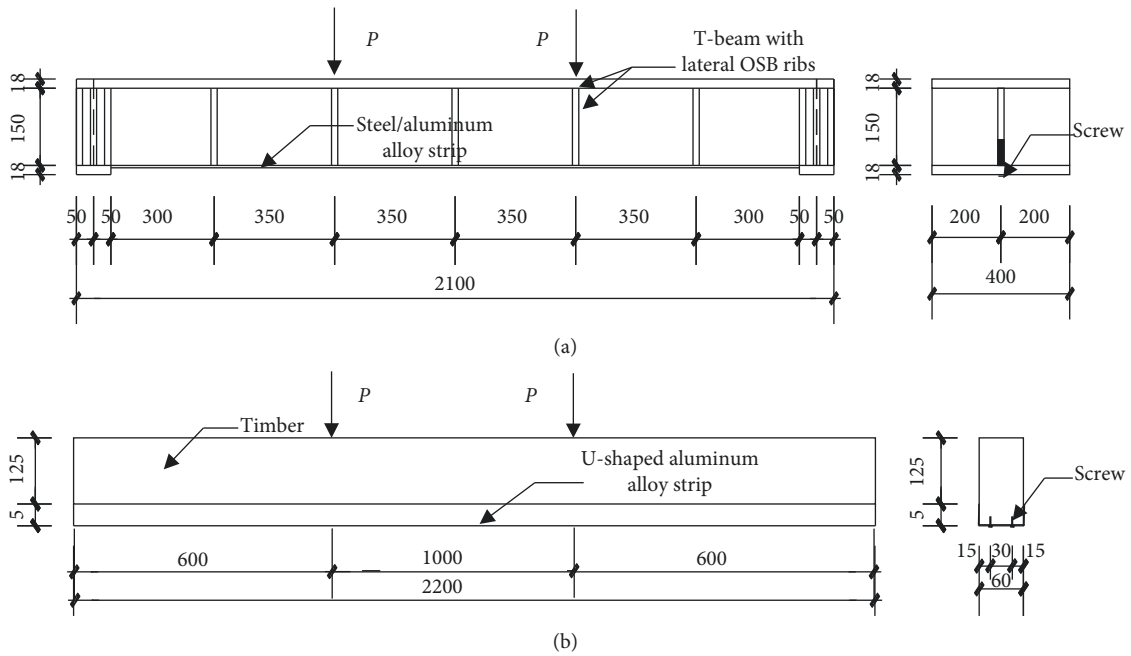

Figure 6: General view of the test: (a) SU-OT beam (mm) [44] and (b) AU-T beam (mm).

the elastic modulus, γ is the Poisson ratio, f_t is the yield strength, and f_c is the compressive strength. Timber simulation based on the trilinear strain-softening constitutive model [45] and the damaged plasticity model was used to describe the behavior of the aluminum alloy. The finite element analysis carried out the AU-T and SU-OT; it also found the modeling method to be effective with which the models were calibrated against the experimental load-deflection data. Then, simulations have done to keep the mechanical properties same and change the flange height of AU-T to 0, 5 mm, 13 mm, 26 mm, 39 mm, 52 mm, and 65 mm and 0, 5 mm, 15 mm, 30 mm, and 45 mm for flange height of SU-OT.

It can be seen that the load-displacement response of AU-T beam simulated by ANSYS in Figure 7 suggested that increasing the flange height of U-shaped member has a significant influence on the stiffness as shown by the decrease trend of displacement at midspan beam with the same load condition. The fitted curves (e.g., Figures 8 and 9) slightly overestimate both AU-T beam and SU-OT beam, and the reduction in maximum displacement and compressive stress indicates providing higher bearing capacity. The curves indicate the flange height of the U-shape member adopted 1/5 beam height that is available, and it is obvious that the carrying capacity would not improve when the height is above 1/5 beam height.

Comparing the carbon fiber-reinforced timber beam, an increase in its carrying capacity is likely to be produced which proved the good behavior of a U-shaped member with fiber-reinforced plastic as well [46–48]. The study [18] does not show the relationship of flange height and carrying capacity, but it can be found that reducing the flange height would be superior for carrying capacity according to the equilibrium and the structure analysis sketch.

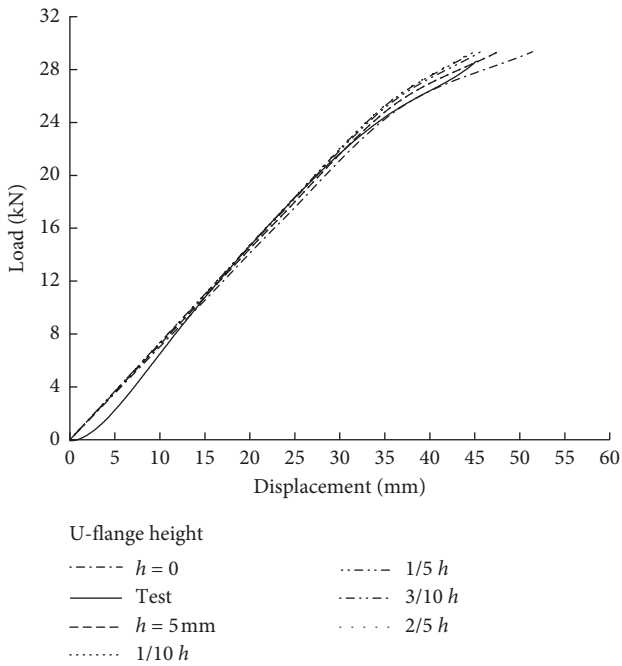

Figure 7: AU-T load-displacement plot.

4. Experiment of Timber Beams Assembled by U-Shaped Member

To check its effectiveness, the thin-layer beam calculation model is compared with the results of experiments on a U-shaped thin-walled strip-timber composite beam. SU-OT [44] and AU-T were analyzed by using both the methods described in this paper and the finite element method. From the data, results of two kinds of timber beam are used for

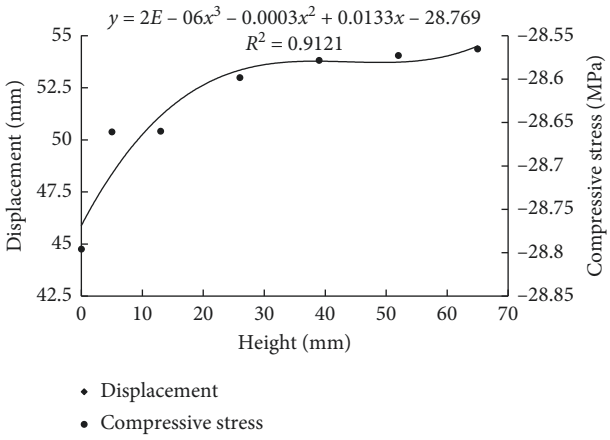

Figure 8: AU-T height-displacement/compressive stress plot.

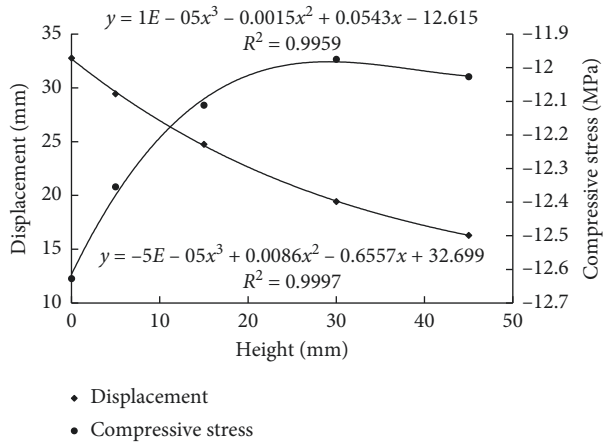

Figure 9: SU-OT height-displacement/compressive stress plot.

discussion here. The general view of SU-OT and AU-T is shown in Figure 6. Specimens made of timber with identical characteristics to the beams in terms of timber origin, quality, drying time, and moisture content were tested. In this case, loads and displacements were obtained, and with this information, the corresponding stress/strain diagrams were traced. The values of the elasticity modulus, maximum compression strength, and Poisson's ratio were presented in Section 3.3.

The tests were conducted at two points of load application, and the displacement of the beams at midspan and at the supports was measured by dial gauges to an accuracy of 0.01 mm. Investigating the details of behavior of the effective load-deflection response of the components was carrying out by several full-scale bending tests in experiments; there was relatively ductile behavior exhibited in load-deflection curves, and the simulation showed very similar results compared to test results. With regard to the load bearing capacity observed in the results for identical models, the effectiveness of parameters used to predict the behavior of beams with different heights of U-shaped flange provided an adequate estimate.

The experimental results are shown in Figures 10 and 11, and comparison of displacement at midspan between calculation and test or simulation using thin layer theory is listed in Table 1. The data obtained correspond to the loads applied and to the vertical midspan displacements experienced by the beams where the load is applied, up to fracture. With these data, load-displacement graphs of the beam were obtained as shown in Figure 7, and the graphs of mean values of the strain under ultimate fracture load are shown in Figures 10 and 11. Figure 10 shows the deformation behavior and strain distribution along the beam, in which the values obtained for the U-shaped member ultimate tensile stress corresponded to coinciding with the maximum compressive stress of timber reached by the reinforcing U shape member. When ultimate load is reached, the tensile stress coinciding with the maximum compressive stress would reach the ultimate point. The structure exhibited a ductile behavior. The load-strain relationship in Figure 11 presented the longitudinal strain along the loading procedure. The results show that there is no occurrence of separation.

It can be seen from Table 1 that the results have shown the ultimate load and corresponding ultimate midspan deflection with calculations by equation (12) and the exact value of simulations. The values of ultimate load indicate fracture load, which was adopted from the experimental data in [49], and conclusion by Pellicane [50] can be applied to the material of aluminum alloy when using the algorithm. In this paper, the K value is 0.3482 for SU-OT and 0.4527 for AU-T. The differences in the results from comparison are less than 5%. The validation is used to check the effectiveness of the numerical model in calculation and simulation of U-shaped member reinforced timber beam. It still needs various experiments for further research and construction application.

5. Conclusions

Accordingly, great effort has been devoted to the development of prototypes of plate strengthening timber hybrid components to be used in composite structure. The U-shaped member combined with timber provides support not only to vertical forces but also to horizontal forces as fractions between interfaces for the failure are triggered by shear slip. Particularly, analysis of timber beams finds that the mild softening part leads the bolts or screws separate before braking by not carrying the vertical load.

Analysis of the mechanical model of interface bond-slip behavior between U-shaped member and timber, and shown in the results of finite element calculation, indicates the U-shape member contributes to the bending capacity, and the available height of flange has been found.

The calculation method based on thin-layer beam theory is validated by numerical analysis that can be used to predict the bending capacity of U-shaped sheet reinforced timber.

The results should be treated as qualitative rather than quantitative due to the small range of data. However, the research for the composite system and the U-shaped member reinforced timber beam still needs to be developed.

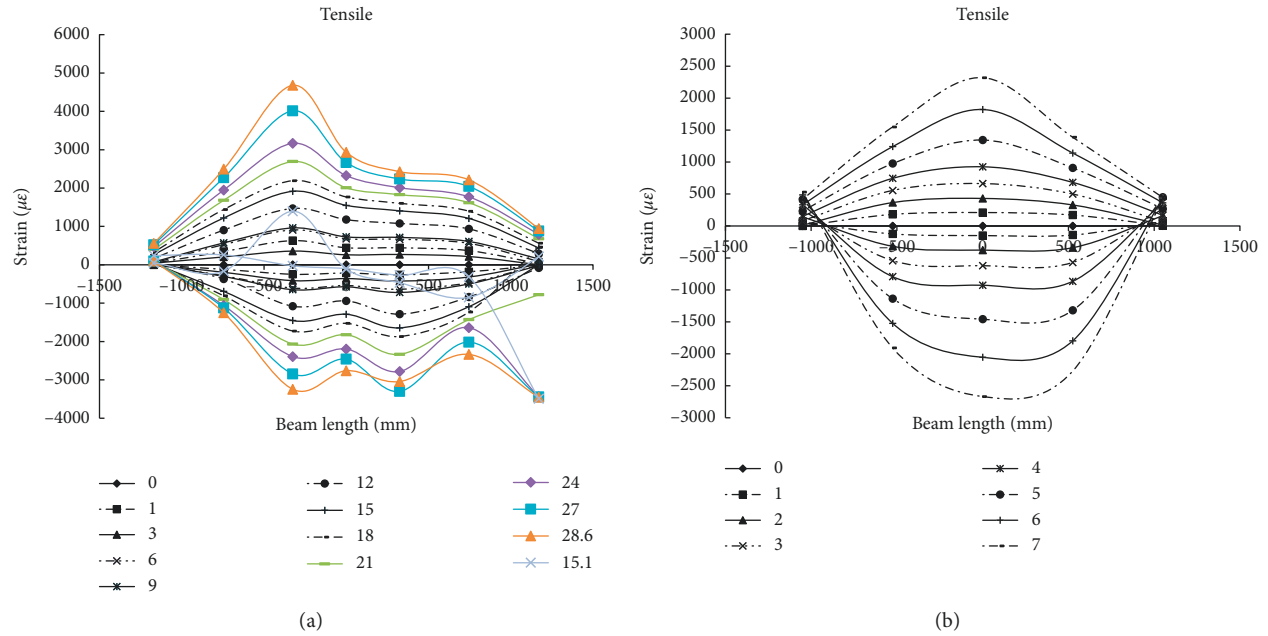

Figure 10: The distribution strain of aluminum alloy sheet and top of timber. (a) AU-T beam. (b) SU-OT beam (mm).

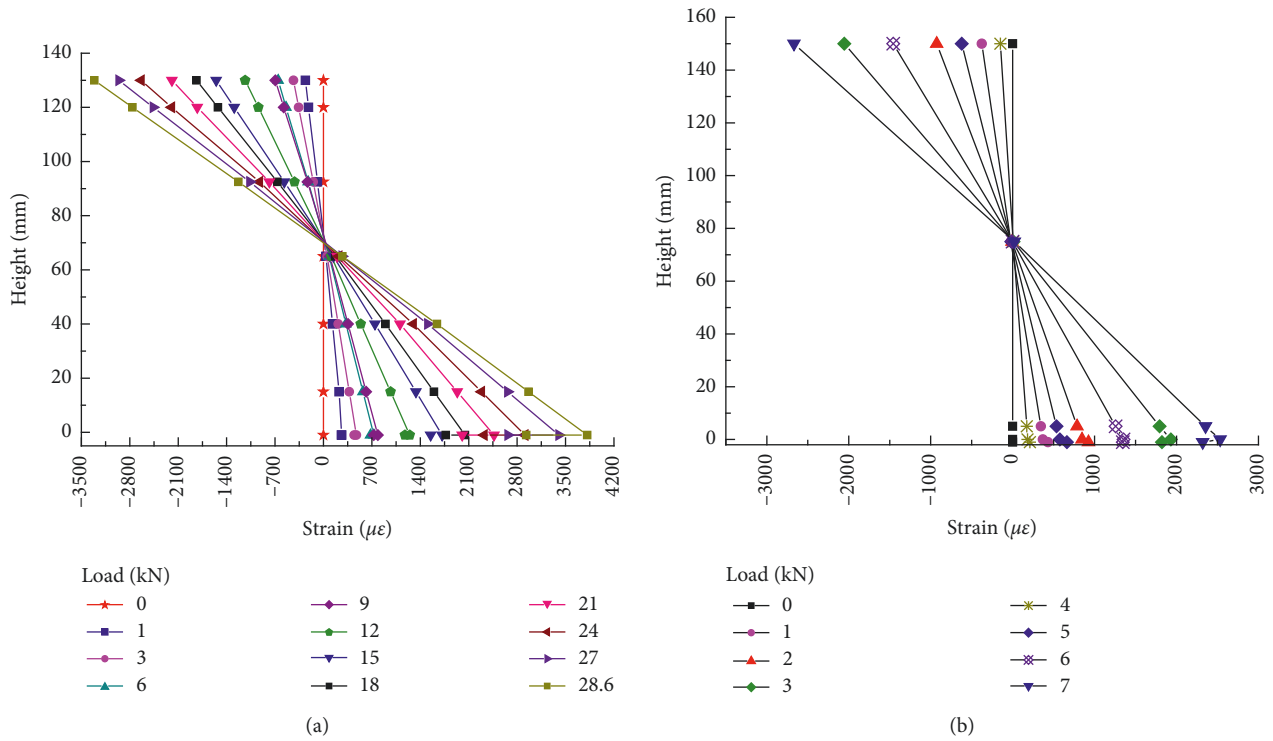

Figure 11: The load-strain curve of specimen section in the middle of the span. (a) AU-T beam. (b) SU-OT beam (mm).

Table 1: Comparison of displacement at midspan between calculation and test or simulation.

No.	Ultimate load in tests (kN)	Displacements in tests (mm)	Calculated displacements (mm)	Error (mm)	Simulation displacements (mm)	Error (mm)
AU-T	28.6	44.31	44.31	0.03	47.60	5.61
SU-OT	7.4	29.70	29.18	1.75	29.46	0.81

Data Availability

The data used to support the findings of this study are available from the corresponding author upon request.

Conflicts of Interest

The authors declare that they have no conflicts of interest.

Acknowledgments

This research was supported by the Hainan Natural and Science Foundation (518MS122 and 518QN307) and the China Postdoctoral Science Foundation (2018M630722).

References

[1] G. A. Howard, *Analysis and Design of Structural Sandwich Panels*, Pergamon Press, Oxford, UK, 1969.

[2] W. K. Edward and L. W. Thomas, "Composite beams effect of adhesive or fastener rigidity," Forest Service Research Paper FPL 152, Forest Products Laboratory, U.S. Department of Agriculture, Madison, WI, USA, 1971.

[3] Y. Liu, E. J. Chen, S.-T. Quek, J.-T. Yi, and F.-H. Lee, "Effect of spatial variation of strength and modulus on the lateral compression response of cement-admixed clay slab," *Géotechnique*, vol. 65, no. 10, pp. 851–865, 2015.

[4] Y. Liu, L. Q. He, Y. J. Jiang, M. M. Sun, E. J. Chen, and F. H. Lee, "Effect of in-situ water content variation on the spatial variation of strength of deep cement-mixed clay," *Géotechnique*, vol. 68, pp. 1–15, 2018.

[5] J. Jasienko and T. P. Nowak, "Solid timber beams strengthened with steel plates–experimental studies," *Construction and Building Materials*, vol. 63, pp. 81–88, 2014.

[6] A. Borri, M. Corradi, and A. Grazini, "A method for flexural reinforcement of old wood beams with CFRP materials," *Composites part B: Engineering*, vol. 36, no. 2, pp. 143–153, 2005.

[7] T. V. A. Nguyen, R. L. Roy, and J. Caron, "Multi-reinforcement of timber beams with composite materials: experiments and fracture modeling," *Composite Structures*, vol. 123, pp. 233–245, 2015.

[8] H. Murakami, "A laminated beam theory with interlayer slip," *Journal of Applied Mechanics*, vol. 51, no. 3, pp. 551–559, 1984.

[9] R. Hussein, "Application of plate theory to laminated wood composites with non-rigid adhesive," *International Wood Products Journal*, vol. 1, no. 1, pp. 35–42, 2013.

[10] H. J. Blaß and P. Schädle, "Ductility aspects of reinforced and non-reinforced timber joints," *Engineering Structures*, vol. 33, no. 11, pp. 3018–3026, 2011.

[11] S. Hay, K. Thiessen, D. Svecova, and B. Bakht, "Effectiveness of GFRP sheets for shear strengthening of timber," *Journal of Composites for Construction*, vol. 10, no. 6, pp. 483–491, 2006.

[12] K. C. Johns and S. Lacroix, "Composite reinforcement of timber in bending," *Canadian Journal of Civil Engineering*, vol. 27, no. 5, pp. 899–906, 2000.

[13] T. C. Triantafillou, "Shear reinforcement of wood using FRP materials," *Journal of Materials in Civil Engineering*, vol. 9, no. 2, pp. 65–69, 1997.

[14] T. W. Buell and H. Saadatmanesh, "Strengthening timber bridge beams using carbon fiber," *Journal of Structural Engineering*, vol. 131, no. 1, pp. 173–187, 2005.

[15] M. Corradi, A. Borri, L. Righetti, and E. Speranzini, "Uncertainty analysis of FRP reinforced timber beams," *Composites Part B: Engineering*, vol. 113, pp. 174–184, 2017.

[16] G. P. De la Rosa, E. A. Cobo, and G. M. N. Gonzalez, "Analysis of the flexural stiffness of timber beams reinforced with carbon and basalt composite materials," *Composites Part B*, vol. 86, pp. 152–159, 2016.

[17] A. M. Malek, H. Saadatmanesh, and M. R. Ehsani, "Prediction of failure load of R/C beams strengthened with FRP plate due to stress concentration at the plate end," *ACI Structural Journal*, vol. 95, pp. 142–152, 1998.

[18] G. P. De la Rosa, E. A. Cobo, and G. M. N. Gonzalez, "Bending reinforcement of timber beams with composite carbon fiber and basalt fiber materials," *Composites Part B*, vol. 55, pp. 528–536, 2013.

[19] F. Rescalvo, I. Valverde-Palacios, E. Suarez, and A. Gallego, "Experimental comparison of different carbon fiber composites in reinforcement layouts for wooden beams of historical buildings," *Materials*, vol. 10, no. 10, pp. 1113–1135, 2017.

[20] F. J. Rescalvo, E. Suarez, C. Abarkane, A. Cruz-Valdivieso, and A. Gallego, "Experimental validation of a CFRP laminated/fabric hybrid layout for retrofitting and repairing timber beams," *Mechanics of Advanced Materials and Structures*, 2018, In press.

[21] A. H. Buchanan, "Bending strength of lumber," *Journal of Structural Engineering*, vol. 116, no. 5, pp. 1213–1229, 1990.

[22] F. H. Theakston, "A feasibility study for strengthening timber beams with fiberglass," *Canadian Agricultural Engineering*, vol. 7, pp. 17–19, 1965.

[23] A. Globa, M. Subhan, J. Moloney, and R. Al-Amen, "Carbon fiber and structural timber composites for engineering and construction," *Journal of Architectural Engineering*, vol. 24, no. 3, article 040808, 2018.

[24] Y. Liu, Y. J. Jiang, H. Xiao, and F. H. Lee, "Determination of representative strength of deep cement-mixed clay from core strength data," *Géotechnique*, vol. 67, no. 4, pp. 350–364, 2017.

[25] M. Subhani, A. Globa, R. Al-Ameri, and J. Moloney, "Flexural strengthening of LVL beam using CFRP," *Construction and Building Materials*, vol. 150, pp. 480–489, 2017.

[26] Y. Liu, F. H. Lee, E. J. Chen, and J. Hu, "Three-dimensional random finite element analysis of cement-admixed soil slab for stabilization of foundation pits," *Chinese Journal of Geotechnical Engineering*, vol. 40, no. 8, pp. 1542–1548, 2018, in Chinese.

[27] J. R. Goodman and E. P. Popov, "Layered beam systems with interlayer slip," *Journal of the Structural Division*, vol. 94, pp. 2535–2548, 1968.

[28] J. R. Goodman and E. P. Popov, "Layered wood systems with interlayer slip," *Wood Science*, vol. 1, pp. 148–158, 1969.

[29] J. R. Goodman, M. D. Vanderbilt, M. E. Criswell, and J. Bodig, "Composite and two-way action in wood joist floor systems," *Wood Science*, vol. 7, pp. 25–33, 1974.

[30] N. M. Newmrk, C. P. Siess, and I. M. Viest, "Tests and analysis of composite beams with incomplete interaction," *Proceedings of the Society for Experimental Stress Analysis*, vol. 9, no. 1, pp. 75–92, 1951.

[31] J. M. Whitney, "Stress analysis of thick laminated composite and sandwich plates," *Journal of Composite Materials*, vol. 6, no. 3, pp. 426–440, 2016.

[32] R. Khandan, S. Noroozi, P. Sewell, and J. Vinney, "The development of laminated composite plate theories: a review,"

Journal of Materials Science, vol. 47, no. 16, pp. 5901–5910, 2012.

[33] H. Liu, B. Z. Cao, X. Zeng, O. Jiasisuo, and H. X. Xu, "Bearing capacity and numerical analysis of timber concrete composite beam with galvanized steel strip," *Natural Science Journal of HaiNan University*, vol. 35, pp. 180–185, 2017.

[34] U. A. Girhammar, "Composite beam-columns with interlayer slip-approximate analysis," *International Journal of Mechanical Sciences*, vol. 50, no. 12, pp. 1636–1649, 2008.

[35] U. A. Girhammar, "A simplified analysis method for composite beams with interlayer slip," *International Journal of Mechanical Sciences*, vol. 51, no. 7, pp. 515–530, 2009.

[36] U. A. Girhammar, D. H. Pan, and A. Gustafsson, "Exact dynamic analysis of composite beams with partial interaction," *International Journal of Mechanical Sciences*, vol. 51, no. 8, pp. 565–582, 2009.

[37] J. G. Nie, J. M. Shen, and Z. W. Yu, "A reduced stiffness method for calculating deformation of steel-concrete composite beams with the consideration of slip effect," *China Civil Engineering Journal*, vol. 28, pp. 11–17, 1995, in Chinese.

[38] U. A. Girhammar and V. K. A. Gopu, "Composite beam–columns with interlayer slip-exact analysis," *Journal of Structural Engineering*, vol. 119, no. 4, pp. 1265–1282, 1993.

[39] J. M. Bai and C. T. Sun, "The effect of viscoelastic adhesive layers on structural damping of sandwich beams*," *Mechanics of Structures and Machines*, vol. 23, no. 1, pp. 1–16, 1995.

[40] C. K. Carlos, A. E. V. Wong, and J. L. Robert, "Shear displacement in open-sandwich reinforced concrete beams," *Magazine of Concrete Research*, vol. 39, no. 139, pp. 83–92, 1987.

[41] R. Hussein, *Composite Panels/Plates-Analysis and Design*, Technomic Publishing Inc., Lancaster, PA, USA, 1986.

[42] J. H. Shen, X. N. Gao, and Q. Y. Zhou, "Influence of slip on deflection of cold-formed thin-walled U-section steel-concrete composite beams," *Journal of Huaqiao University*, vol. 30, pp. 557–562, 2009, in Chinese.

[43] Y. Xiao, L. W. Peng, and S. Kunnath, "Analysis of composite beams with interlayer slip," *Journal of Hunan University (Natural Sciences)*, vol. 44, pp. 77–86, 2017, in Chinese.

[44] C. R. Zhu, "The Experimentl study on flexural behavior of cold-formed steel-OSB board composite beam," Mater Thesis, Hainan University, Haikou, China, 2017, in Chinese.

[45] J. Y. Luo, X. Li, and R. Z. Deng, "Numerical analysis on flexural performance of a new kind timber-steel composite beams," *Low Temperature Architecture Technology*, vol. 39, pp. 46–48, 2017.

[46] F. J. Rescalvo, E. Suarez, I. Valverde-Palacios, J. M. Santiago-Zaragoza, and A. Gallego, "Health monitoring of timber beams retrofitted with carbon fiber composites via the acoustic emission technique," *Composite structures*, vol. 206, pp. 392–402, 2018.

[47] F. Rescalvo, I. Valverde-Palacios, E. Suarez, A. Roldán, and A. Gallego, "Monitoring of carbon fiber-reinforced old timber beams via strain and multiresonant acoustic emission sensors," *Sensors*, vol. 18, no. 4, p. 1224, 2018.

[48] P. Alam, M. P. Ansell, and D. Smedley, "Mechanical repair of timber beams fractured in flexure using bonded-in reinforcements," *Composites Part B: Engineering*, vol. 40, no. 2, pp. 95–106, 2009.

[49] Y. Z. Yang, "Study on the properties of the light-gauge steel truss girder-OSB composite floor," Mater Thesis, Chongqing University, Chongqing, China, 2014, in Chinese.

[50] P. J. Pellicane and J. Bodig, "Comparison of nailed joint test methods," *Journal of Testing and Evaluation*, vol. 12, no. 5, pp. 261–267, 1984.